Proc. Natl. Acad. Sci. USA
Vol. 96, pp. 10062–10067, August 1999
Biochemistry

Crystal structure of triosephosphate isomerase from *Trypanosoma cruzi* in hexane

XIU-GONG GAO*, ERNESTO MALDONADO*, RUY PÉREZ-MONTFORT*, GEORGINA GARZA-RAMOS*, MARIETTA TUENA DE GÓMEZ-PUYOU*, ARMANDO GÓMEZ-PUYOU*, AND ADELA RODRÍGUEZ-ROMERO†‡

*Instituto de Fisiología Celular and †Instituto de Química, Universidad Nacional Autónoma de México, 04510 México D. F., Mexico

Edited by Alexander M. Klibanov, Massachusetts Institute of Technology, Cambridge, MA, and approved July 1, 1999 (received for review May 11, 1999)

ABSTRACT **To gain insight into the mechanisms of enzyme catalysis in organic solvents, the x-ray structure of some monomeric enzymes in organic solvents was determined. However, it remained to be explored whether the structure of oligomeric proteins is also amenable to such analysis. The field acquired new perspectives when it was proposed that the x-ray structure of enzymes in nonaqueous media could reveal binding sites for organic solvents that in principle could represent the starting point for drug design. Here, a crystal of the dimeric enzyme triosephosphate isomerase from the pathogenic parasite *Trypanosoma cruzi* was soaked and diffracted in hexane and its structure solved at 2-Å resolution. Its overall structure and the dimer interface were not altered by hexane. However, there were differences in the orientation of the side chains of several amino acids, including that of the catalytic Glu-168 in one of the monomers. No hexane molecules were detected in the active site or in the dimer interface. However, three hexane molecules were identified on the surface of the protein at sites, which in the native crystal did not have water molecules. The number of water molecules in the hexane structure was higher than in the native crystal. Two hexanes localized at <4 Å from residues that form the dimer interface; they were in close proximity to a site that has been considered a potential target for drug design.**

Recently, there has been increasing interest in the x-ray structure of enzymes in organic solvents (1–10). In these studies, there have been essentially two objectives. One is to ascertain the structural basis that allows enzymes to express in organic solvents properties that differ drastically from those observed in conventional aqueous media (11). The other is to identify binding sites for organic molecules, because theoretically, these regions could represent potential sites for structure-based inhibitor and drug design (5, 12). To date, the x-ray structures of subtilisin, elastase, and lysozyme in acetonitrile (1, 5, 9), subtilisin in dioxane (6), γ-chymotrypsin in hexane (3, 4), and β-trypsin in cyclohexane (10) have been successfully determined. In some cases, the crystallized enzyme had to be mildly cross-linked before its exposure to organic solvents and collection of diffraction data (1, 2, 5, 9). All of these enzymes are monomers. Thus, it was considered of interest to explore whether the x-ray structure of oligomeric enzymes also could be determined in organic solvents. To this end, we used triosephosphate isomerase (TIM) from *Trypanosoma cruzi* (TcTIM), the parasite that causes Chagas' disease, which affects more than 20 million people in the Americas. As shown here, we obtained the crystal structure of TcTIM in hexane at a resolution of 2 Å. Thus, it was possible to ascertain the impact that organic solvents have on the structure of a dimeric enzyme.

The publication costs of this article were defrayed in part by page charge payment. This article must therefore be hereby marked "*advertisement*" in accordance with 18 U.S.C. §1734 solely to indicate this fact.

PNAS is available online at www.pnas.org.

Regarding potential sites for drug design, x-ray studies of oligomeric enzymes in organic solvents also seemed worthwhile. This is because most of the enzymes that have been targeted for drug development in parasitic diseases are oligomeric enzymes (13–17). Along this line, it is relevant that TIMs from *T. cruzi* (18), *Trypanosoma brucei* (14, 19), and *Plasmodium falciparum* (20) have been considered targets for drug design, respectively, against Chagas' disease, sleeping sickness and nagana in Africa, and malaria which has worldwide distribution.

TIM is a homodimer that catalyzes the interconversion of glyceraldehyde 3-phosphate and dihydroxyacetone phosphate. The kinetics, catalytic mechanisms, and energetics of the reaction have been thoroughly studied (21, 22). Crystallographic data of TIM from several different species at good resolution levels are also available (19, 20, 23–28). The TIM monomers are formed by eight β-strands joined to eight α-helices (numbered 1–8) by the corresponding loops.

MATERIALS AND METHODS

Crystallization and Soaking of Crystal in Hexane. Crystals from recombinant TcTIM(18) were obtained at room temperature by the hanging-drop diffusion method in 0.1 M Hepes (pH 7.5), 2% (vol/vol) PEG 400, and 2.0 M $(NH_4)_2SO_4$ (23). One crystal was placed in a thin-walled quartz capillary tube; the aqueous solution was removed with filter paper. The tube was flushed thoroughly with *n*-hexane dehydrated with 4-Å molecular sieves. The hexane-filled tube was placed for 24 h in a capped bottle that contained hexane and molecular sieves; thereafter, it was sealed and mounted on a goniometer head for data collection.

Data Collection and Processing. Diffraction data were collected at 18°C on an R-AXIS IIC imaging plate detector in a Rigaku rotating anode x-ray generator. Data were reduced with the DENZO/SCALEPACK package (29). Structure factor magnitudes were truncated by using the CCP4 program suite (30). Table 1 summarizes the results.

Refinement. The starting model was native TcTIM (PDB ID code 1tcd) without water molecules. Refinement calculations were made with X-PLOR (31); 10% of the reflections were randomly selected for cross-validation. Model building and correction were performed with QUANTA (Molecular Simulations, Waltham, MA). Three rounds of simulated annealing were performed; resolution was increased in each round. Before dynamics, 80 cycles of conjugated gradient minimiza-

This paper was submitted directly (Track II) to the *Proceedings* office.
Abbreviations: TcTIM, triosephosphate isomerase from *Trypanosoma cruzi*.
Data deposition: The atomic coordinates have been deposited in the Protein Data Bank, www.rcsb.org (PDB ID codes 1ci1 and r1ci1sf).
‡To whom reprint requests should be addressed at: Instituto de Química, Universidad Nacional Autónoma de México, Circuito Exterior, Ciudad Universitaria, 04510 México D.F., Mexico. E-mail: adela@servidor.unam.mx.

Table 1. Statistics for data collection, reduction, and refinement

Data collection and reduction	
Space group	$P2_12_12_1$
Unit cell dimension, Å	$a = 43.7$, $b = 77.7$, $c = 149.2$
Total number of reflections	172,135
Unique reflections	31,766
Resolution, Å	2.0
Completeness, %	84.4
R_{merge} %	11.6
V_m (Å^3·Da^{-1})	2.3
Redundancy	3.6
Refinement	
Number of hexane molecules	3
Number of water molecules	236
Resolution range for refinement, Å	5.0–2.0
Number of reflections in the refinement	26,956
R/R_{free}; %	18.1/23.6
rms deviation (bond/angle/torsion)	0.006 Å/1.2°/25.0°
Mean B factor (protein/hexane/water), Å	24.4/51.5/33.6

tion were used to relieve bad contacts. The system was heated to 3,000 K and cooled to 300 K in 25-K decrements. The time for molecular dynamics was 0.5 fs. Conventional positional and B factor refinements followed simulated annealing refinement in each macrocycle. $(2F_o - F_c)$ and $(F_o - F_c)$ maps showed continuous long densities that could be attributed to hexanes; these were built manually into the map and tested for short contacts before their incorporation. Parameters and topology files for hexane were obtained from the Protein Data Bank. Water molecules were built into the model with X-SOLVATE within QUANTA. Initially, 14 hexanes and 52 waters were included in the model. Eight more refinement cycles were made. In each cycle, torsion-angle molecular dynamics slow cool refinement was conducted at a starting temperature of 5,000 K, followed by conventional positional and B factor refinement. After each cycle, $(2F_o - F_c)$ and $(F_o - F_c)$ maps were prepared to verify the existence of hexanes and for building new waters. The maps for some hexanes deteriorated with progressive refinements, and simulated annealing omit maps were calculated at the positions of these hexanes to further verify their existence. Two of the initial 14 hexanes were successfully retained after the final cycle of refinement; a third hexane was built into the model after the eighth cycle. The total number of waters was 236. Table 1 shows the resulting data.

RESULTS

We soaked TcTIM crystals in acetonitrile and in dioxane, but this resulted in disruption of the crystals. However, crystals of TcTIM resisted repeated washing with hexane, incubation with hexane for 24 h, and collection of diffraction data in hexane for 36 h.

General Features of the Hexane Structure. In hexane**,** the structure of the dimer was conserved. The Cα trace of the hexane structure superposed very closely with that of the native enzyme (Fig. 1). The rms deviation of the Cα backbone between the dimer in hexane and the native enzyme was 0.15 Å. In the crystal structure of native TcTIM (23), loops six of monomers A and B are in the closed and open conformations, respectively; these conformations were conserved in the hexane structure.

Hexane Molecules. In the hexane structure of TcTIM, three hexane molecules (H1, H2, and H3) were identified (Fig. 1)**,** none of which was at the active site. The buried portion of the dimer interface was also free of hexane molecules. The three hexane molecules were at the surface of TcTIM. In the native structure, the regions of the protein that bound hexane did not contain water molecules.

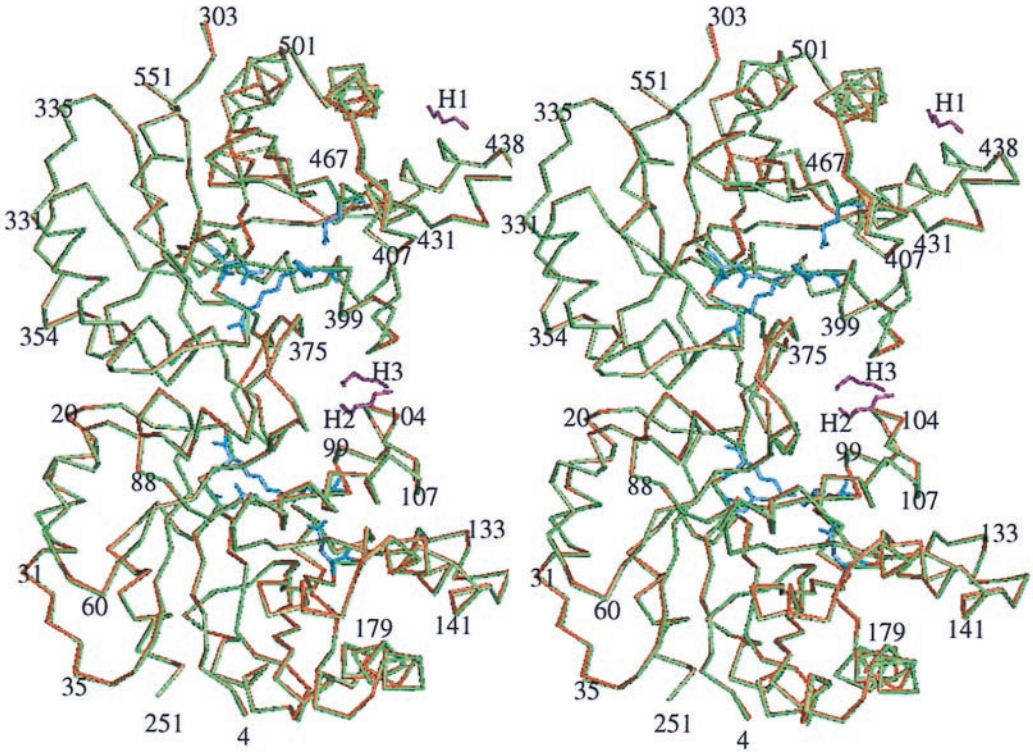

FIG. 1. Stereoview of the Cα traces of the hexane (red) and native (green) structures. The catalytic residues in each of the two subunits of the hexane structure are in blue. Numbers 1–251 and 301–551 indicate the amino acids of monomers A and B, respectively. The three hexane molecules (H1, H2, and H3) are in purple.

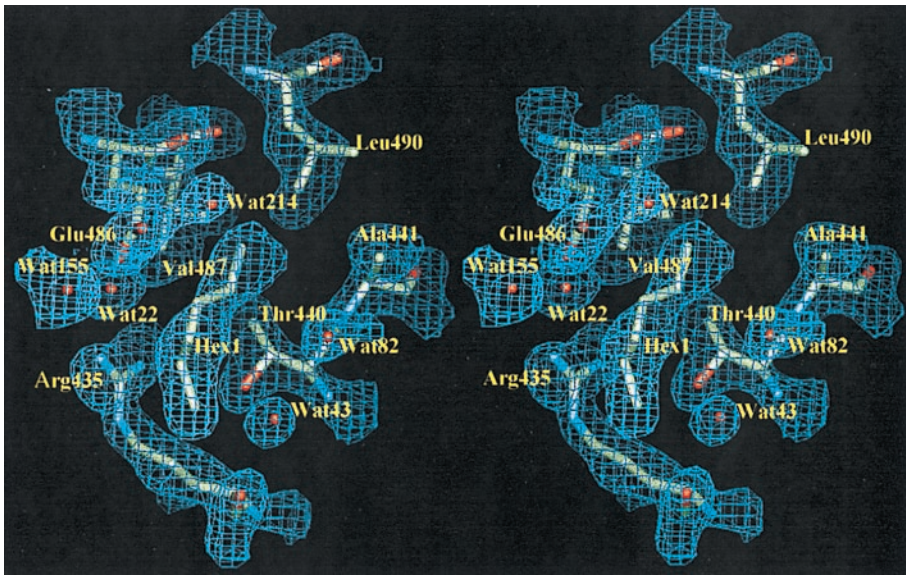

FIG. 2. Stereoview of the $(2F_o - F_c)$ map contoured at 1σ of H1. The carbon, nitrogen, and oxygen atoms are represented in cyan, blue, and red, respectively.

H1 was located at <4 Å from residues Arg-135, Thr-140, and Glu-186 of subunit B Fig. 2); these residues form part of loop 5 and helix 6. H2 and H3 were 3.8 Å from each other. They localized in a hydrophobic patch that is formed by residues of the two subunits (Fig. 3). H2 was <4 Å from Ile-69, Tyr-103, Gly-104, Ile-109, and Lys-113 of monomer A and from Tyr-102 and -103 of monomer B. H3 also situated at <4 Å from residues in the two subunits: Phe-75 from subunit A and Tyr-102 and -103 from subunit B.

Catalytic Sites. In view of the different activities that some enzymes exhibit in organic solvents and in water (11), the x-ray structure of the catalytic centers has received considerable attention. In all enzymes thus far studied (1–10), organic-solvent molecules appear at the active site. However, in TcTIM, no hexane molecules were observed in either of its two catalytic sites. Another feature of the x-ray reports on enzymes in organic solvents is that the geometry of catalytic residues does not undergo drastic changes.

The catalytic residues in TcTIM are Asn-12, Lys-14, His-96, and Glu-168 of the same monomer. The former two fix the substrate at the active site, whereas His-96 and Glu-168 participate in proton transfer between glyceraldehyde 3-phosphate and dihydroxyacetone phosphate (21, 22). Asn-12, Lys-14, and His-96 superpose almost exactly in the native and hexane structures with an rms difference of 0.15 Å. In monomer B, Glu-168 also had the same geometry in the two structures, but in monomer A, the orientation of the side chain of Glu-168 was significantly different (Fig. 4). The χ 1, 2, and 3 angles of Glu-168 in the water structure were 19, 113, and $-78°$, respectively; in the hexane structure, they were 33, 151,

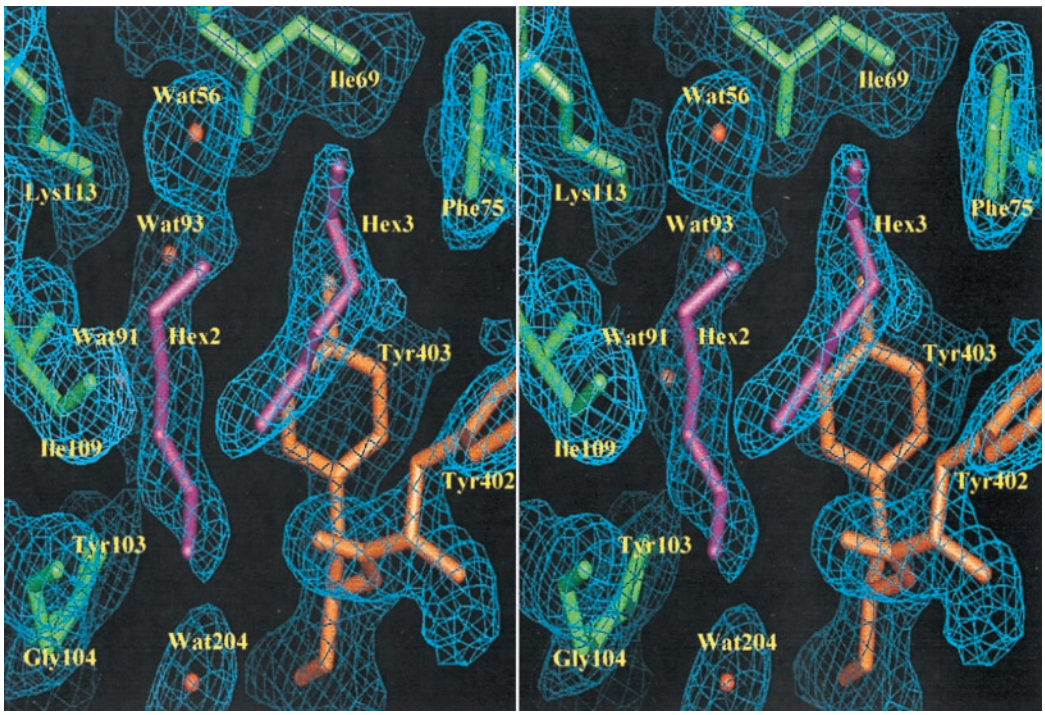

FIG. 3. Stereoview of the $(2F_o - F_c)$ map contoured at 1σ of H2, H3, and surrounding residues. The residues of subunits A and B are shown in green and orange, respectively. H2 and H3 are in purple, and waters are in red.

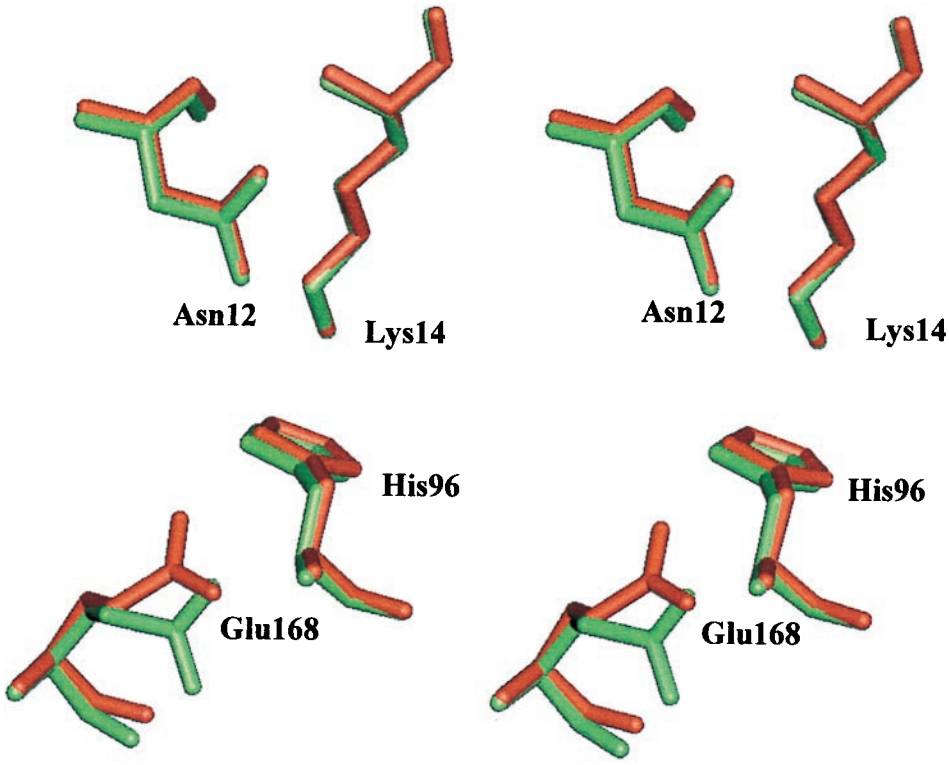

FIG. 4. Stereoview of the superposition of the four catalytic site residues from monomers A of the hexane (red) and native (green) structures.

and −146°. The diffraction pattern was of good quality in both structures. The change in the orientation of the side chain of the catalytic Glu-168 could have important implications in catalysis, because its substitution by an aspartate affects strongly the kinetics of the enzyme (32).

The different orientation of the side chain of Glu-168 of monomer A most likely reflects a long-range effect of hexane. This could be related to the existence of hexane in only one of the two equivalent regions of the protein or to the different conformation that loop 6 has in the two monomers. However, it is noted that there is transmission of events from the catalytic sites to the region of the interface formed between Cys-15 of one monomer and loop 3 of the other monomer (33). Thus, the existence of two hexane molecules at <4 Å from Ile-69 and Phe-75 of loop 3 might be a coincidence, or it may indicate a perturbation transmitted from loop 3 to Glu-168.

Water Molecules. In native TcTIM, 165 water molecules were identified. In the hexane structure, there were 236. Of the water molecules in the native enzyme, 127 were conserved, Thus, hexane caused the displacement of 38 water molecules and the appearance of 109 in places where no water molecules had been detected. Zaks and Klibanov (34) showed that in organic solvents, the catalytic integrity of enzymes increases with the hydrophobicity of the solvent, and that this was related to the ability of the solvent to remove water from the protein. Therefore, the enrichment of water in the hexane structure would result from energetic barriers that prevent the partition of water from the protein into the hydrophobic solvent.

Effect of Hexane on the Orientation of the Side Chains of TcTIM. In the enzymes that have been exposed to organic solvents, some of the side chains of the amino acids undergo changes in orientation (1–10); these are more frequent in residues that are close to the organic-solvent molecules. In the hexane structure of TcTIM, the side chain of Ile-109 of monomer A, which is close to H2, underwent such a change. However, there were also changes in residues that were far from the hexane molecules. In total, we detected clear deviation from the native structure in 19 residues. An interesting alteration is that of Asp-86 of monomer A; it is part of helix 3 and is in front of Glu-19 of the other subunit. These two residues form the most external part of the interface. In the hexane structure, there was a significant deviation of the side chain of Asp-86 (Fig. 5). No other significant modifications were observed in the 58 residues that participate in the intersubunit contacts of TcTIM. In fact, the solvent-accessible area of the hexane structure was 19,272 $Å^2$, whereas that of the native enzyme is 19,101 $Å^2$.

B Factors. It has been proposed that enzymes are rigidified in organic solvents (35). Although there are reports that indicate relative low B factors on enzymes in organic solvents (1), others show that these thermal factors are not modified (3, 5). In TcTIM, the average B factors of the hexane and native structures were 24.4 and 22.5 $Å^2$, respectively. However, B factors depend on the resolution of crystal and the refinement procedure; thus, the two values cannot be strictly compared.

DISCUSSION

Most of the work on the x-ray structure of enzymes in organic solvents has been accompanied by reports of their catalytic properties in nonaqueous solvents (for review, see ref. 36). Measurements of TIM activity require a trapping enzyme; because the properties of the latter enzyme are probably affected in nonaqueous media, it would be difficult to obtain accurate kinetic data when TIM is placed in such conditions. Therefore, we limited our studies to the x-ray structure of TcTIM in hexane and the identification of hexane-binding sites.

One of the implications of our results is that the x-ray structure of complex oligomeric enzymes can be determined in nonaqueous solvents. In this respect, a noteworthy feature of the data is that in hexane, the general structure of the TcTIM dimer, including its subunit interface, is strikingly similar to that of the enzyme in the native crystal. The marked similarity in the two enzymes is strongly suggestive that the hexane-binding sites are not artifacts induced by hexane but that

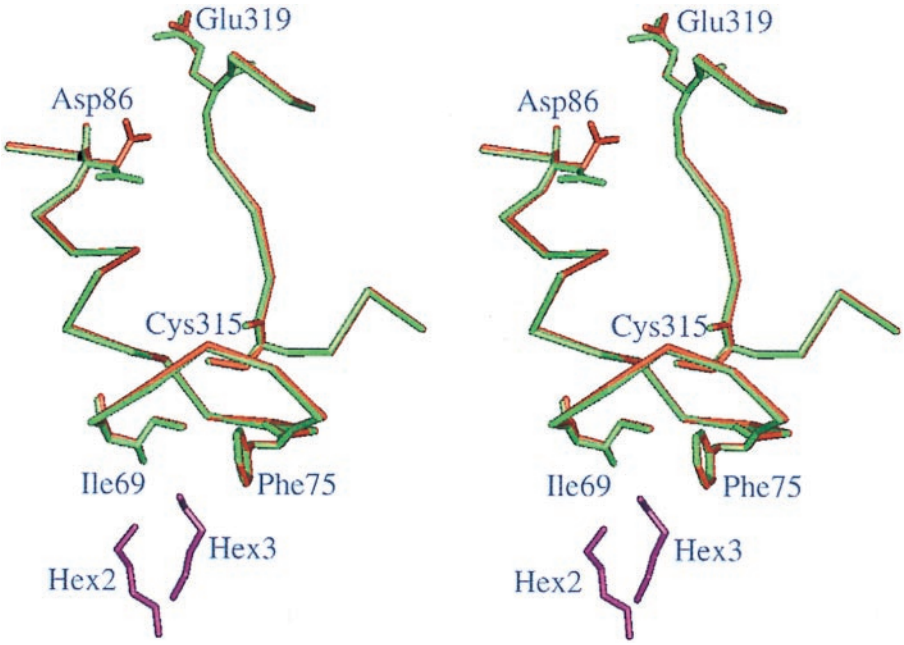

FIG. 5. Stereoview of the Cα trace of the interface region near H2 and H3 in the hexane and native structures. All atoms of the indicated residues are shown. Colors are as in Fig. 1. Note that the numbering of the residues in subunit A is from 1 to 251, and in subunit B from 301 to 551.

indeed they represent true binding sites for nonpolar molecules that exist in native TcTIM.

Nonetheless, hexane-induced changes in orientation of the side chains of several amino acids. These findings are in consonance with data on monomeric enzymes that show that organic solvents do not perturb the basic structure of proteins but nevertheless cause changes in the geometry of the side chains of some residues (1–10). In TcTIM, it is noted, however, that although the enzyme is a homodimer, the changes induced by hexane did not occur in the two monomers; for example, changes in the orientation of the side chain of Asp-86 and the catalytic Glu-168 appeared in only one of the two monomers. Furthermore, H1 was found only in monomer B. The causes of the differences between the two monomers are not clear, but structural differences between two equivalent regions of TIM have been described. In TcTIM, for example, there is a clear difference in the separation at the beginning of the interface between loop 1 of one monomer and helix 3 of the other monomer in the two equivalent regions of the dimer (23).

Because subunit interfaces have been considered potential sites for drug design (37, 38), a salient feature of the results is that H2 and H3 are in a hydrophobic patch that lies on the outer portion of the interface. As shown in Figs. 3 and 5, the two hexanes were at <4 Å from residues of the two subunits; two of these residues (Ala-69 and Phe-75) belong to loop 3 of subunit A. The residues of the latter loop (69–80) surround the side chain of Cys-15 of the other subunit (Fig. 5). Several lines of evidence indicate that the interactions of the side chain of residue 15 with loop 3 are central in dimer stability and enzyme catalysis (39–41); along this line, it is noted that the derivatization of Cys-15 by thiol reagents produces drastic irreversible structural alterations and abolition catalysis (39, 40). Because human TIM has a methionine in position 15, it has been suggested that this region of the enzyme can be targeted for species specific inhibition of TcTIM (23, 39, 40). In fact, TcTIM is completely inhibited by sulfhydryl reagents at concentrations that hardly affect human TIM or TIMs that lack a cysteine in position 15 (42). In this context, it is relevant that H2 and H3 are also in proximity to Tyr-103 of monomer A and Tyr-102 and -103 of monomer B (Fig. 3). In human TIM, Tyr-102 and -103 are replaced by valine and phenylalanine, respectively. Therefore, it may be feasible to design molecules that interact specifically with TcTIM in this critical region of the enzyme.

This work was supported by grants from Consejo Nacional de Ciencia y Tecnología and Dirección General de Asuntos del Personal Académico de la Universidad Nacional Autónoma de México. X-ray data set was collected at Laboratorio Univrsitario de Estructura de Proteinas, Instituto de Quimica, UNAM.

1. Fitzpatrick, P. A., Steinmetz, A. C. U., Ringe, D. & Klibanov, A. M. (1993) *Proc. Natl. Acad. Sci. USA* **90**, 8653–8657.
2. Fitzpatrick, P. A., Ringe, D. & Klibanov, A. M. (1994) *Biochem. Biophys. Res. Commun.* **198**, 675–681.
3. Yennawar, N. H., Yennawar, H. P. & Farber, G. K. (1994) *Biochemistry* **33**, 7326–7336.
4. Yennawar, H. P., Yennawar, N. H. & Farber, G. K. (1995) *J. Am. Chem. Soc.* **117**, 577–585.
5. Allen, K. N., Bellamicina, C. R., Ding, X., Jeffery, C. J., Mattos, C., Petsko, G. A. & Ringe, D. (1996) *J. Phys. Chem.* **100**, 2605–2611.
6. Schmitke, J. L., Stern, L. J. & Klibanov, A. M. (1997) *Proc. Natl. Acad. Sci. USA* **94**, 4250–4255.
7. Schmitke, J. L., Stern, L. J. & Klibanov, A. M. (1998) *Biochem. Biophys. Res. Commun*. 248, 273–277.
8. Schmitke, J. L., Stern, L. J. & Klibanov, A. M. (1998) *Proc. Natl. Acad. Sci. USA* **95**, 12918–12923.
9. Wang, Z., Zhu, G., Huang, Q., Qian, M., Shao, M., Jia, Y. & Tang, Y. (1998) *Biochim. Biophys. Acta* **1384**, 335–344.
10. Zhu, G., Huang, Q., Wang, Z., Qian, M., Jia Y. & Tang, Y. (1998) *Biochim. Biophys. Acta* **1429**, 142–150.
11. Westcott, C. R. & Klibanov, A. M. (1994) *Biochim. Biophys. Acta* **1206**, 1–9.
12. Ringe, D. (1995) *Curr. Opin. Struct. Biol.* **5,** 825–829.
13. McTigue, M. A., Williams, D. R. & Tainer, J. A. *J. Mol. Biol.* **246**, 21–27 (1995).
14. Fairlamb, A. H. & Cerami, A. (1992) *Annu. Rev. Microbiol.* **46**, 695–729.
15. Verlinde, C. L. M. L, Merrit, E. A., Van Den Akker, F., Kim, H., Feil, I., Delboni, L. F., Mande, S. C., Sarfaty, S., Petra, P. H. & Hol, W. G. J. (1994) *Protein Sci.* **3**, 1670–1686.
16. Read, J. A., Wilkinson, K. W., Tranter, R., Sessions, R. B. & Brady, R. L. (1999) *J. Biol. Chem.* **274**, 10213–10218.
17. Phillips, C., Dohnalek, J., Gover, S., Barrett, M. P. & Adams M. J. (1998) *J. Mol. Biol.* **282**, 667–681.
18. Ostoa-Saloma, P., Garza-Ramos, G., Ramírez, J., Becker, I., Berzunza, M., Landa, A., Gómez-Puyou, A., Tuena de Gómez-

Puyou, M. & Pérez-Montfort, R. (1997) *Eur. J. Biochem*. **244**, 700–705.
19. Wierenga, R. K., Noble M. E. M. & Davenport, R. C. (1992) *J. Mol. Biol.* **224**, 1115–1126.
20. Velanker, S. S., Ray, S. S., Gokhale, R. S., Suma, S., Balaram, H., Balaram, P. & Murthy, M. R. N. (1997) *Structure (London)* **5**, 751–761.
21. Albery, W. J. & Knowles, J. R. (1976) *Biochemistry* **15**, 5631–5640.
22. Harris T. K., Cole R. N., Comer F. I. & Mildvan A. S. (1998) *Biochemistry* **37**, 16828–16838.
23. Maldonado, E., Soriano-García. M., Moreno, A., Cabrera, N., Garza-Ramos, G., Tuena de Gómez-Puyou, M., Gómez-Puyou, A. & Pérez-Monfort, R. (1998) *J. Mol. Biol.* **283**, 193–203.
24. Lolis, E. Alber, T., Davenport, R. C., Rose, D., Hartman, F. C. & Petsko, G. A. (1990) *Biochemistry* **29**, 6609–6618.
25. Mande, S. C., Mainfroid, V., Kalk, K. H., Goraj, K., Martial, J. A. & Hol, W. G. (1994) *Protein Sci.* **3**, 810–821.
26. Alber, T., Banner, D. W., Bloomer, A. C., Petsko, G. A., Philips, D. C., Rivers, P. C. & Wilson, I. A. (1981) *Philos. Trans. R. Soc. London Ser. B* **293**, 159–171.
27. Noble, M. E. M., Zeelen. J. P., Wierenga, R. K., Mainfroid, V., Goraj, K., Gohimont, A. C. & Martail, J. A. (1993) *Acta Crystallogr. D* **49**, 403–417.
28. Delboni, L. F., Mande, S. C., Rentier-Delrue, F., Mainfroid, V., Turley, S., Vellieux, F. M. D., Martial, J. A. & Hol, W. G. J. (1995) *Protein Sci.* **4**, 2594–2604.
29. Otwinowski, Z. & Minor, W. (1997) *Methods Enzymol.* **276**, 307–326.
30. Bailey, S. (1994) *Acta Cystallogr. D* **50**, 760–763.
31. Brunger, A. T. (1992) X-PLOR: *A System for X-Ray Crystallography and NMR* (Yale Univ. Press, New Haven, CT), Version 3.1.
32. Raines, R. T., Sutton, E. L., Straus, D. R., Gilbert, W. & Knowles, J. R. (1986) *Biochemistry* **25**, 7142–7154.
33. Perez-Montfort, R., Garza-Ramos, G., Hernández-Alcantara, G., Reyes-Vivas, H., Gao, X.-G., Maldonado, E., Tuena de Gómez-Puyou, M. & Gómez-Puyou, A. (1999) *Biochemistry* **38**, 4114–4120.
34. Zaks, A. & Klibanov, A. M. (1988) *J. Biol. Chem.* **263**, 8017–8021.
35. Klibanov, A. M. (1989) *Trends Biochem. Sci.* **14**, 141–144.
36. Tuena de Gómez-Puyou, M. & Gómez-Puyou, A. (1998) *Crit. Rev. Biochem. Mol. Biol.* **33,** 53–89.
37. Zutshi, R., Brickner, M. & Chmielewski, J. (1998) *Curr. Opin. Chem. Biol.* **2**, 62–66.
38. Prasanna, V., Bhattacharjya, S. & Balaram, P. (1998) *Biochemistry* **37**, 6883–6893.
39. Gomez-Puyou, A., Saavedra-Lira, E., Becker, I., Zubillaga, R. A., Rojo-Domínguez. A. & Pérez-Montfort, R. (1995) *Chem. Biol.* **2**, 847–855.
40. Garza-Ramos, G., Cabrera, N., Saavedra-Lima, E., Tuena de Gómez-Puyou, M., Ostoa-Saloma, P., Pérez-Montfort, R. & Gómez-Puyou, A. (1998) *Eur. J. Biochem.* **253,** 684–691.
41. Mainfroid, V., Terpstra, P., Beauregard, M., Frere, J.-M., Mande, S. C., Hol, W. G. J., Martial, J. A. & Goraj, K. (1996) *J. Mol. Biol.* **257,** 441–456.
42. Garza-Ramos, G., Pérez-Montfort, R., Rojo-Domínguez, A., Tuena de Gómez-Puyou, M. & Gómez-Puyou, A. (1996) *Eur. J. Biochem.,* **241,** 114–120.